

Flotation separation of cassiterite and chlorite using carboxymethyl cellulose as a depressant

Yang Hu ^{1,2}, Luo Hong Ying ³, Ying Zhang ¹, Lu Kuan Wei ¹, Guan Zhen Hao ¹

¹ Kunming University of Science and Technology

² Zijin Mining Group Co., Ltd.

³ Panzhihua Iron and Steel Research Institute Co.

Corresponding authors: zhyingcsu@163.com (Ying Zhang)

Abstract: The nature and mechanism of interaction between carboxymethyl cellulose (CMC) with cassiterite (and chlorite surfaces) and their effects on the flotation separation process of cassiterite (from chlorite) were investigated by micro-flotation tests, surface adsorption experiments, zeta potential measurements, solution chemical calculation, infrared spectroscopy, and X-ray photo-electron spectroscopy (XPS). The results from single mineral tests revealed that CMC exhibited good selective inhibition effects with cassiterites and chlorites. When the dosage was 12.5 mg/L at pH 8, cassiterite and chlorite recovery was 92.2% and 6.3%, respectively. The artificial mixed ore test revealed that the flotation separation effect was the best when the dosage of CMC was 6.5 mg/L. Cassiterite used during the studies was 75.1% pure. The recovery was 82.8%. The interaction between CMC and the cassiterite surface led to a shift in the zeta potential toward the negative direction. CMC was weakly adsorbed on the cassiterite surface. There was no significant impact on the subsequent collection of sodium oleate. The concentration of C atom increased post interaction, and the potential shifted toward the negative direction. Characteristic CMC peaks were observed at this point. Hydrogen bonds and weak chemisorption interactions between CMC and chlorite affected the interaction between sodium oleate and the chlorite surface. It also affected the flotation results. The cassiterite and chlorite were separated effectively.

Keywords: cassiterite, chlorite, sodium oleate, carboxymethyl cellulose, selective inhibition

1. Introduction

Tin is a rare element. The percentage of tin in the earth's crust is only 0.004% (Je et al., 2014; Fuliang et al., 2014). The mineral composition is complex in various tin deposits. The associated components (such as quartz, calcite, pyrrhotite, chlorite, etc.) can be found in higher amounts. At present, tin can be mainly found in cassiterite (SnO₂) (reaching 75.0%). It is estimated that cassiterite contains 78.8% of tin. Pure cassiterite is quite rarely (Angadi et al., 2015). With the development of the flotation technology and the increased economic exploitation of low-grade ore deposits, the flotation of fine and ultra-fine particles has become particularly important (Waters et al., 2008; George et al., 2004). Chlorite is a gangue mineral exhibiting a negative impact on the quality of tin concentrate. Therefore, it is necessary to study the flotation separation techniques with cassiterite and chlorite. The biggest impact of chlorite on cassiterite recovery was that chlorite easily formed slime on the surface of cassiterite, affecting the grade of the cassiterite concentrate (Chen et al., 2018; Feng et al., 2018; Qicheng et al., 2018; Beattie et al., 1992; Wei et al., 2015). The mutual attraction of the two led a large amount of chlorite to adhere to the surface of cassiterite. They float together under the action of a collector, resulting in the decline of the quality of tin concentrate. Ordinary reagents cannot effectively separate cassiterite from chlorite (Sun et al., 2001). However, the floatability of chlorite increased with the increase in pH when sodium oleate was used as the collector (Chen et al., 2018). So, it is necessary to study the flotation separation of cassiterite and chlorite. It is very important to separate cassiterite from chlorite by selective inhibition of reagents. At the same time, the study of the flotation behavior of cassiterite and chlorite also has practical applicability.

Fatty acids and their salts exhibit good cassiterite collecting properties. Sodium oleate (NaOL) is one of the commonly used collectors in the cassiterite flotation process. During the flotation process, it gets adsorbed on the surface of the oxidized ore (by the method of complexation or combination) to realize the collection of minerals. In addition, sodium oleate exhibits strong collection ability but the adsorption value of sodium oleate is low (Sun et al., 2001; Agnes 1965; Lyubimov et al., 1963; Amp 2012). Due to the weak selectivity of sodium oleate, depressants are needed to inhibit the gangue minerals in the pulp during flotation (Feng et al., 2018). The common depressants used are the inorganic depressants (sodium silicate, sodium sulfide, sodium hexametaphosphate, etc.) and organic inhibitors (carboxymethyl cellulose, starch, citric acid, dextrin, etc.). Sodium silicate, sodium hexametaphosphate, starch, and other depressants could inhibit cassiterite in the flotation process (Bulatovic, 2015). They can potentially affect the recovery index of cassiterite. CMC (carboxymethyl cellulose) is a commonly used organic depressant for cassiterite flotation (Bulatovic, 2015; Ejtemaia, 2012). CMC inhibits calcium and magnesium silicate through electrostatic adsorption, hydrogen bonding, chemical adsorption, and surface interactions (Burdukova et al., 2008). The carboxyl and hydroxyl groups of the molecules provide protons to form hydrogen bonds with the oxygen atoms on the mineral surface (Ejtemaia, 2012). Some polar groups present in CMC get adsorbed on the mineral surface (Burdukova et al., 2008). The other hydroxyl groups associate with water (through hydrogen bond) to make the mineral surface hydrophilic. CMC interacts with minerals containing metal ions (such as chlorite, serpentine, and amphibole) via electrostatic interactions and chemical adsorption (between carboxyl and metal ions) (Burdukova et al., 2008; Ejtemaia, 2012; Burdukova et al., 2008; Zhang, 2010; Bulatovic, 2015; Wang and Somasundam, 2005). CMC can also get adsorbed on the surface of the minerals. CMC can change the surface electrical properties of the minerals (attractive to repulsive interaction). It also exhibits a certain dispersion effect on pulp (Wang and Somasundam, 2005; Beattie et al., 2006).

In this paper, the flotation separation technique of cassiterite and chlorite has been studied (pure mineral flotation test). The effects of CMC on the flotation behavior of cassiterite and chlorite have been investigated with sodium oleate as the collector and sodium hydroxide and sulfuric acid as the regulators. There are a few reports on the flotation separation technique of cassiterite and chlorite. Chlorite is one of the main gangues of cassiterite and their efficient separation is necessary to obtain high-quality tin. The effects of CMC on the flotation of cassiterite and chlorite and its selectivity mechanism have been explored using the chemical calculation of flotation solution, zeta potential test (Feng et al., 2012), infrared spectroscopy, X-ray photoelectron spectroscopy (XPS) techniques, etc. With depleting tin deposits and therefore smaller amounts of cassiterite available, this method can make more efficient use of resources. An important theoretical basis for the separation and recovery of the same type of minerals has also been explained.

2. Experimental

2.1. Sample preparation

Pure cassiterite and chlorite were collected in Yunnan Province, China. X-ray diffraction and X-ray fluorescence analyses showed that these samples were of high purity. After crushing and hand-selected purification, deionized water was used to rinse and dry the surface of the mineral (at room temperature), and then a three-head agate grinder was used for initial grinding, and a standard screen was used to fully screen the ground mineral samples. $-74\mu\text{m}$ was used for flotation test, and $-18\mu\text{m}$ was used for detection. The potentiodynamic measurements were performed and infrared spectra were recorded using samples with a particle size of $-18\mu\text{m}$. The tin ore contained 75.1% tin. The purity was 98.6%, which met the requirements of the test. The XRD test results are shown in Fig. 1. The XRD spectrum of chlorite is shown in Fig. 2. The amount of impurity minerals was low. The purity was more than 90%, which met the requirements for the test.

2.2. Test reagent

The main chemicals used in the test, their chemical formulae, purity, and manufacturer from whom they were obtained are shown in Table 1. Deionized water was used during the experiments. Sodium oleate was employed as anionic collector of cassiterite and chlorite. Hydrochloric acid (0.1 mol/L) and

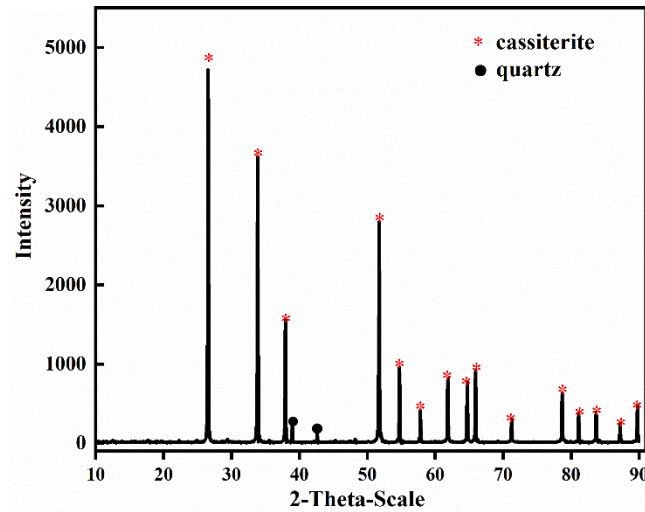


Fig. 1. XRD pattern of the pure cassiterite samples

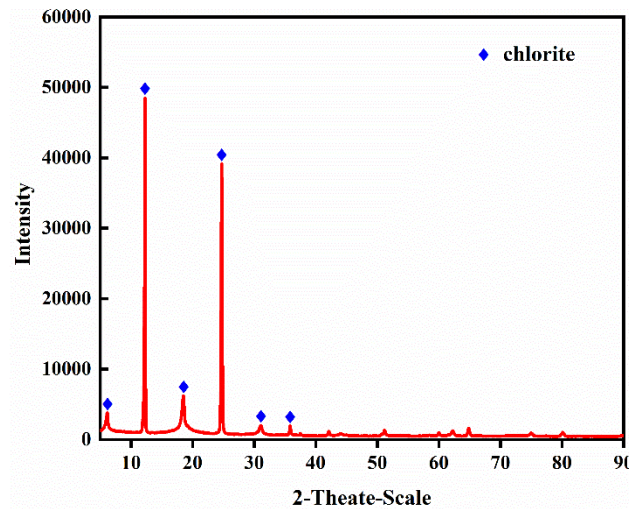


Fig. 2. XRD pattern of the pure chlorite samples

Table 1. Main test reagents.

Name	Molecular Formula	Purity	Manufacturer
Sodium oleate	$C_{18}H_{33}NaO_2$	Analytically pure	Tianjin Guangfu Fine Chemical Research Institute
sodium hydroxide	NaOH	Analytically pure	Tianjin FengChuan chemical reagent Technology Co., Ltd.
sulfuric acid	H_2SO_4	Analytically pure	Tianjin Damao Reagent Factory
Carboxymethyl cellulose	$C_6H_7O_2(OH)_2CH_2COOH$	Analytically pure	Tianjin kemeo Chemical Reagent Co., Ltd.

sodium hydroxide (0.1 mol/L) stock solutions were used to adjust the solution pH in the experiments. Pure deionized water with a resistivity of 18 MΩ produced by a Milli Q50 system (Billerica, MA, USA) was used throughout the experimental work

2.3. Research methods

2.3.1. Single mineral flotation test

The 40 mL XFG hanging cell flotation machine operated at a speed of 1600 r/min was used for the experiments (artificially mixed ore: cassiterite and chlorite mixed in the mass ratio of 1:1; Sn grade of

mixed ore: 39.9%). The flow chart is shown in Fig. 3. The concentration of sodium oleate was 1.5×10^{-4} mol/L. The test temperature was approximately 25 °C. The pure mineral sample (2.0 g) was weighed into a 40 mL flotation cell. An appropriate amount of deionized water was added to it and the mixture was stirred for 2 min. Following this, sulfuric acid or sodium hydroxide was added to the reaction mixture to adjust the pulp pH to the specified value. Subsequently, the depressant was added and the mixture was stirred for 3 min. Finally, we added the collector, after three minutes of action, flotation scraping bubble. It was floated for another 3 min. Finally, the products that settled at the bottom (and the product that floats up) were filtered, dried, and weighed. The amount of substance recovered was estimated. The experiment was repeated thrice and the average value was reported.

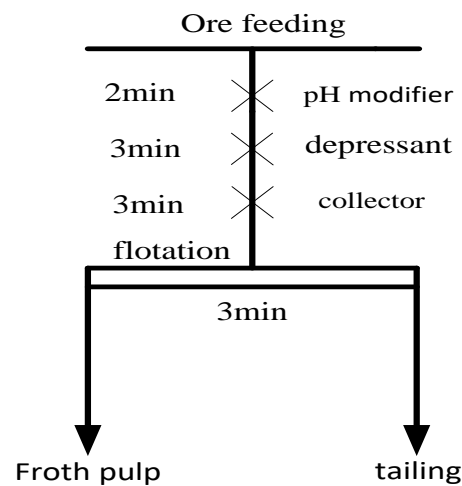


Fig. 3. Flow chart of pure mineral flotation method

2.3.2. Zeta potential measurements

Zeta potential was calculated using the Zetasizer nano Zs90 system developed by Malvern (England). The pure mineral was ground with agate mortar until the particle size was less than 2 μm . During the test, 0.1 g of the sample was weighed and placed in a beaker. A volume of 40 ml of the respective electrolyte concentration was added into the beaker. The appropriate reagent was added and the reaction mixture was stirred for 10 min. A suitable amount of the suspension was pipetted out and put into the electrophoresis cell. The potential measurement tests were conducted. The experiments were repeated thrice under the same conditions. The average value was reported.

2.3.3. Fourier transform infrared spectroscopy (FTIR)

In an agate mortar, the ore sample was ground until the particle size was less than 2 μm . The ore sample (1.0 g) and an appropriate amount of deionized water were put into the beaker and the sample was dispersed in it. The mixture was ultrasonicated for 1 min. Hydrochloric acid and sodium hydroxide were added to the solution to adjust the pulp pH. An appropriate amount of chemicals were added to the solution and stirred for another 30 min. After the solid and liquid phases were separated, the supernatant was dried at 40 °C in a vacuum drying oven. The dried samples and potassium bromide powder were ground and mixed using an agate mortar. The produced sample was put into the tablet press for sample processing. The samples were characterized using the Nicolet FTIR-740 Fourier transform infrared spectrometer (400 cm^{-1} to 4000 cm^{-1}).

2.3.4. X-ray photoelectron spectroscopy (XPS)

XPS data were recorded using a PHI5000 Versa Probe II instrument (PHI5000, ULVAC-PHI, Japan) using an Al $K\alpha$ X-ray source under an ultrahigh vacuum. The survey scan detected all the elements present in the samples. The high-resolution XPS spectra of the target element were recorded. All spectra were calibrated according to the C1s spectrum at a binding energy of 284.8 eV (for charge compensation).

Samples for XPS measurements were prepared as follows: 1.0 g of the mineral samples were dispersed into 50 mL of the aqueous solution. The pulp pH was adjusted by adding hydrochloric acid and sodium hydroxide stock solutions. CMC and sodium oleate solutions were added as required and the reaction mixture was conditioned for 30 min. The samples were collected, dried, and stored for XPS analysis.

3. Results and discussion

3.1. The effect of CMC on the floatability of cassiterite and chlorite

The flotation recovery of cassiterite and chlorite at different pH values are shown in Fig. 4 (sodium oleate dosage: 1.5×10^{-4} mol/L). It can be seen from the Fig. that cassiterite exhibits good floatability in neutral and weak alkaline environments. In the pH range of 7–8, the flotation recovery of cassiterite was approximately 87.0%. The flotation recovery of chlorite was very low in the sodium oleate system in acidic pH. In an alkaline environment, its recovery increased with the increase of pH. The recovery of chlorite was 29.3% at pH 8. In conclusion, the floatabilities of cassiterite and chlorite were low in acidic pH. The floatability of cassiterite was the maximum in a weak alkaline environment. The floatability of chlorite was better in a strongly alkaline environment.

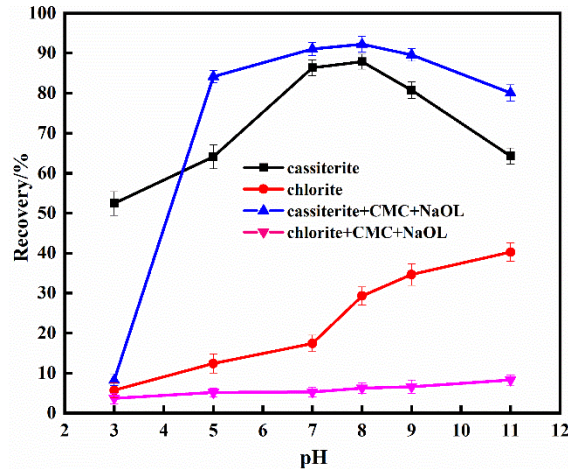


Fig. 4. Floatability of cassiterite and chlorite as a function of pH (sodium oleate dosage: 1.5×10^{-4} mol/L, CMC dosage: 12.5 mg/L)

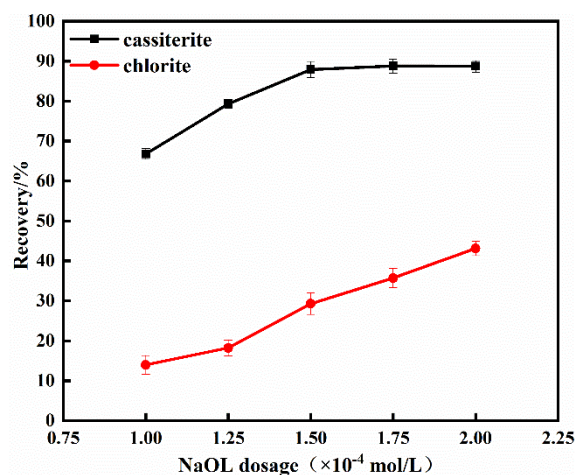


Fig. 5. Floatability of cassiterite and chlorite as a function of sodium oleate concentration at pH = 8

The relationship between flotation recovery of cassiterite (and chlorite) and pH are shown in Fig. 4 (sodium oleate dosage: 1.5×10^{-4} mg/L, CMC dosage: 12.5 mg/L). It can be seen from the Fig. that the recovery of chlorite was less than 10% and that of cassiterite was approximately 80.0% in the whole pH

range. The recovery of cassiterite was above 80% when pH was in the range of 5–11. When the pH of the solution increased to 8, the flotation recovery of cassiterite was 92.3%, which was 85.9% different from chlorite.

As shown in Fig. 5, the recovery of cassiterite increased with the increase in the sodium oleate dosage. When the dosage of sodium oleate was 1.5×10^{-4} mol/L, cassiterite recovery was 87.9%. When the sodium oleate dosage was greater than 1.5×10^{-4} mol/L, the cassiterite recovery value became constant. With the increase of sodium oleate dosage, the recovery of chlorite increased. When the dosage was 1.5×10^{-4} mol/L, the recovery of chlorite was 29.3%. When the sodium oleate dosage was increased to 2.0×10^{-4} mol/L, the chlorite recovery was 43.1%.

It can be seen from Figs. 4 and 5 that the recovery of cassiterite and chlorite increased with the increase of sodium oleate dosage. When sodium oleate dosage was 1.5×10^{-4} mol/L, cassiterite recovery was 87.9% and chlorite recovery was 29.3% at pH 8. The flotation recovery difference between the two was 58.6%. The addition of depressants could further increase the difference in the floatability.

The effects of CMC dosage on the floatability of cassiterite and chlorite are shown in Fig. 6, at a sodium oleate dosage of 1.5×10^{-4} mol/L at pH = 8. When the CMC concentration increased from 0 to 25 mg/L, the chlorite recovery decreased from 29.3% to 2.0%. The recovery of cassiterite did not change significantly with the increase in CMC concentration. When the dosage of CMC increased from 0 to 50 mg/L, the cassiterite recovery decreased from 88.4% to 86.7%. The addition of CMC produced a good selective depressant effect on the two minerals. The addition of appropriate amounts of CMC could effectively separate cassiterite from chlorite.

When the solution pH was in the range of 7–8 and sodium oleate was used as the collector, the separation effect of cassiterite and chlorite is not significant. However, chlorite can be effectively separated from cassiterite by adding CMC. It indicated that the addition of an appropriate amount of CMC could effectively separate cassiterite from chlorite. Based on these observations, cassiterite and chlorite were mixed at a mass ratio of 1:1 (the Sn grade of the mixed ore was 39.9%). The flotation separation behavior of cassiterite and chlorite was observed in the absence of a depressant by adding different amounts of CMC. The result is shown in Fig. 7.

When the pH was in the range of 7–8, and sodium oleate dosage was 1.5×10^{-4} mol/L, the flotation results (tin grade: 60.12%) exhibited a recovery of 85.2% in the absence of a depressant. The flotation separation between cassiterite and chlorite improved with the addition of CMC. When the dosage of CMC was 6.5 mg/L, the yield of the mixed flotation froth was 43.9%, the Sn grade was 75.1%, and the recovery was 82.8%. In the absence of a depressant, the quality of Sn increased, but the recovery decreased by 2.4%. With an increase in the CMC concentration, the recovery percentage for Sn increased. When the CMC dosage was 18 mg/L, the grade of Sn did not change, but the recovery decreased to 46.8%. Therefore, cassiterite and chlorite can be efficiently separated when the CMC dosage was 6.5 mg/L.

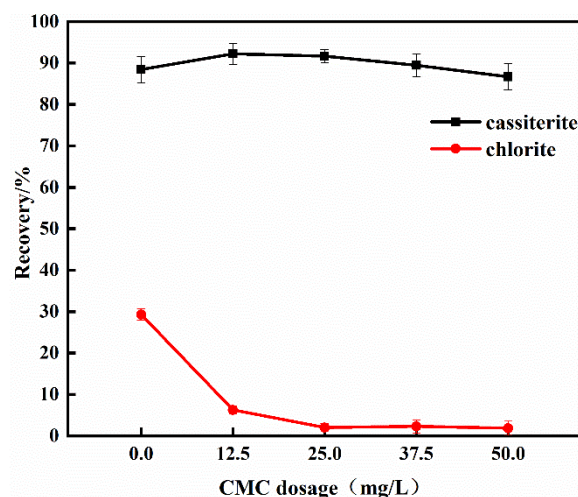


Fig. 6. Effect of CMC concentration on the flotation behavior of cassiterite and chlorite.

[sodium oleate] = 1.5×10^{-4} mol/L at pH = 8

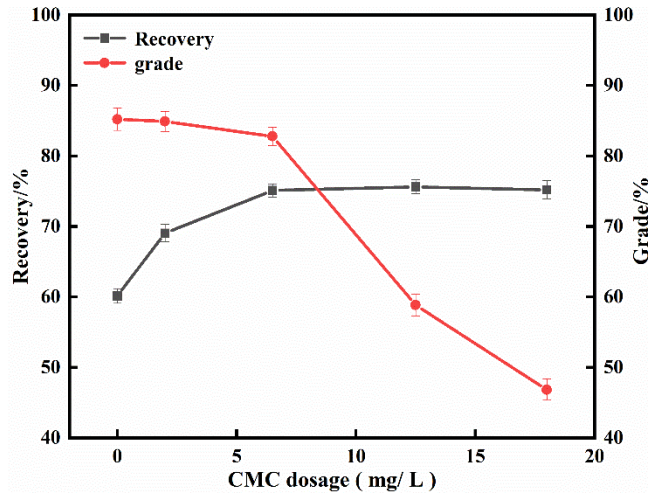


Fig. 7. Flotation separation test results of cassiterite and chlorite

3.2. Zeta potential measurement

The solution composition diagram of cassiterite is shown in Fig. 8 (Qicheng et al., 1992). The solution of cassiterite contained various tin containing hydroxyl compounds formed by the interaction between the cassiterite surface and water. The concentrations of Sn(OH)_3^+ , Sn(OH)_2^{2+} , Sn(OH)^{3+} , and Sn^{4+} decreased with the increase in pH (till a certain pH). The concentrations of Sn(OH)_5^- and Sn(OH)_6^{2-} increased with the increase in pH. The surface of cassiterite was positively charged at $\text{pH} < 4.5$. Tin mainly exists in the form of Sn^{4+} , Sn(OH)^{3+} , Sn(OH)_2^{2+} , and Sn(OH)_3^+ in solution. At $\text{pH} < 7.6$, tin mainly exists in the form of Sn(OH)_3^+ , Sn(OH)_5^- , and Sn(OH)_6^{2-} in solution. When $\text{pH} > 7.6$, Sn(OH)_5^- and Sn(OH)_6^{2-} are the main components in the solution. According to the flotation test, Sn(OH)_5^- and Sn(OH)_6^{2-} were the effective components at $\text{pH} = 8$.

The main components in the sodium oleate solution were HOL , HOL (aq) , $(\text{OL})_2^{2-}$, OL^- , and H(OL)_2^- (Fig. 9). Under strongly acidic conditions, sodium oleate mainly exists in the form of oleic acid. With the increase in pH, the content of oleic acid molecules gradually decreases. The main components of the sodium oleate solution were $(\text{OL})_2^{2-}$ and OL^- when pH was greater than 8.36. In a strong alkaline environment, the number of hydroxyl ions is significantly high. The hydroxyl ions compete with the anions of oleic acid to adsorb or hinder the formation of the oleic acid molecular ion association complex, reducing the collectibility of sodium oleate. Under strongly acidic conditions, sodium oleate mainly exists in oleic acid, which cannot easily react with the mineral surface. It was observed that $(\text{OL})_2^{2-}$ and OL^- were the effective components of sodium oleate in the flotation of cassiterite.

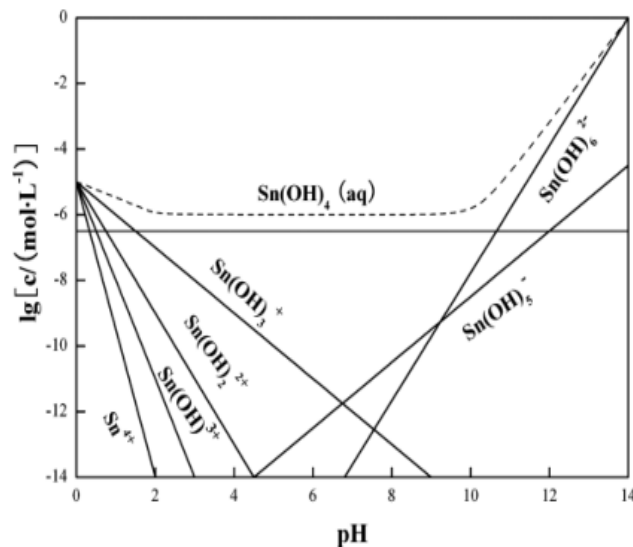


Fig. 8. Distribution diagram of surface species on cassiterite as a function of pH

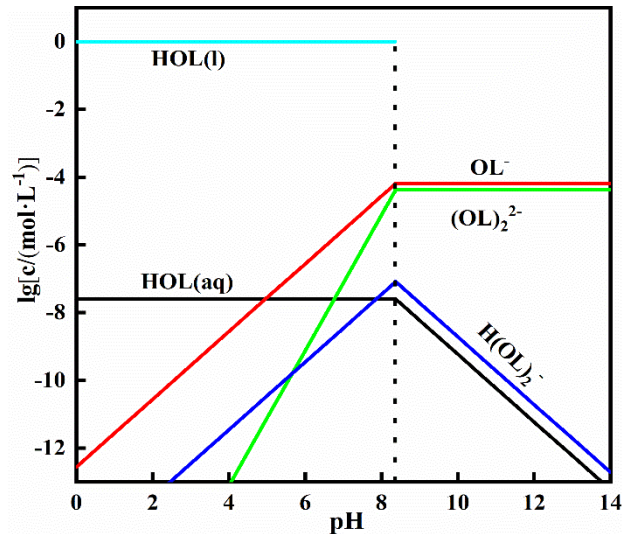


Fig. 9. Species distribution diagram of sodium oleate as a function of pH

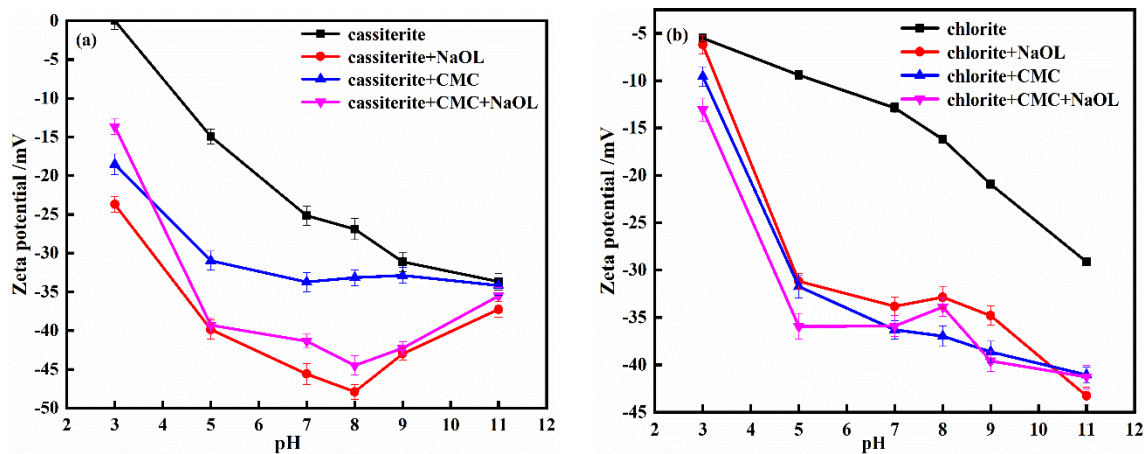


Fig. 10. (a) Effect of sodium oleate and CMC on the zeta potential of cassiterite as a function of pH; (b) Effect of sodium oleate and CMC on the zeta potential of chlorite as a function of pH

Zeta potential is a helpful tool for determining the interaction of flotation reagents with mineral surfaces in the pulp solution. The pH of the solution greatly influenced the surface charge of the mineral particles. The zeta potentials of cassiterite and chlorite were measured within a wide pH range in the absence and presence of CMC (with sodium oleate as the collector, Fig. 10).

As shown in Fig. 10, the zeta potential of bare cassiterite particles decreased with increasing pulp pH. The isoelectric point (IEP) of bare cassiterite was achieved at pH 3. In the absence of any reagent, the content of $\text{Sn}(\text{OH})_3^+$ gradually decreased and the content of $\text{Sn}(\text{OH})_5^-$ progressively increased with the increase in pH. The electronegativity of the cassiterite surface gradually increased and the potential continuously shifted to the negative region. When sodium oleate was added to the solution, the potential decreased significantly (<8) at pulp pH. The zeta potential of cassiterite was the most negative (-47.9 mV), which indicated that the maximum amount of sodium oleate was present on the cassiterite surface at pH = 8. The dominant components of the sodium oleate solution were OL^- and $(\text{OL})_2^{2-}$ although they were electrostatically repelled by the cassiterite surface. The interaction energy between the OL^- ion and the main crystal surface exposed on the cassiterite surface was -268.86 kJ/mol, stronger than the interaction energies between H_2O (and OH^-) with the cassiterite surface (-184.05 kJ/mol and -238.16 kJ/mol, respectively) (Qin et al., 2012; Gong et al., 2018). The results revealed that OL^- can replace OH^- and H_2O . When pH > 8, the potential of cassiterite became negative due to the increase in the negative charge on the cassiterite surface. The electrostatic repulsion between cassiterite and sodium

oleate increased with the increase in cassiterite's negative surface charge. Thus, the adsorption of sodium oleate on the cassiterite surface decreased. This was consistent with the flotation results.

It can be seen from Fig. 10b that the zeta potential of bare chlorite particles decreases with increasing pulp pH. The zeta potential of the chlorite surface shifts continuously to the negative side when the pH value increases. The value was smaller than that of the chlorite surface containing sodium oleate in deionized water. The results revealed that sodium oleate is adsorbed on the surface of chlorite. This changes the number of charged ions on the surface of chlorite.

Both the surfaces of cassiterite and chlorite were negatively charged (from the perspective of surface electrical properties of minerals) and repel each other in the presence of the anionic sodium oleate collector at pH 8. It can be seen from Fig. 10 that the surface potential of cassiterite and chlorite becomes more negative when sodium oleate is chemically adsorbed on the surface of cassiterite and chlorite. The zeta potential of the cassiterite surface was smaller than that of the cassiterite surface containing CMC. The adsorption of CMC on cassiterite results in the change in the number of charged ions on the surface of cassiterite. The decrease in the absolute potential value in acidic pH was greater than that in alkaline pH. The inhibitory effect of CMC on cassiterite was stronger in acidic conditions and the inhibition effect was mainly due to micellar electrostatic adsorption. When $\text{pH} > 5$, the potential of cassiterite continuously decreased with the increase in pH. When $\text{pH} = 11$, the potential difference was close to zero, which indicated that the extent of CMC adsorption on the cassiterite surface decreased with the increase in pH. Both cassiterite and CMC surfaces were negatively charged. The electrostatic repulsion between them reduced the extent of CMC adsorption on the cassiterite surface with the best pulp pH. Thus, the inhibition effect weakened. The surface potential of chlorite became negative with the increase in pH (Fig. 10b). The change in value was larger than that in cassiterite. In acidic pH (less than the pK_a value of CMC), chlorite exhibited micellar electrostatic adsorption. When pulp pH was less than 5, the continuous dissociation of CMC led to an increase in the concentration of the carboxyl anions. Meanwhile, the electrostatic repulsion was not significant enough to prevent the interaction between CMC and the local points on the surface of chlorites.

CMC, to some extent, can cause the generation of negative surface potential. However, CMC significantly affected the zeta potential of chlorite. The decrease in the chlorite potential was considerably greater than cassiterite at pH 8 because the surface potential of chlorite was corrected relative to cassiterite. Local positive and negative charges were present on the surface of chlorite that promoted the interactions between the chlorite and carboxyl anions. CMC produced significant selective inhibition on chlorite.

The zeta potential of cassiterite changed significantly due to the interaction between CMC and sodium oleate. However, the change was similar to that observed for chlorite. The results revealed that the surface potential of cassiterite and chlorite exhibited a negative shift due to interaction. Compared to the surface potential of cassiterite, in the presence of sodium oleate, the surface potential of CMC and sodium oleate exhibited a small positive shift indicating that the introduction of CMC weakened the adsorption of sodium oleate on the surface of cassiterite. However, the intensity of the action was small. At the same time, it was also observed that CMC did not significantly react with the surface of cassiterite. Due to the interaction between CMC and sodium oleate, the chlorite potential exhibited a negative shift (compared with sodium oleate). It indicated that both CMC and sodium oleate were adsorbed on the surface of chlorite. The negative charge on the surface of the debris increased. To sum up, the interaction between CMC and the cassiterite surface was weaker than that with the chlorite surface, which exhibited a selective inhibition for the two minerals. The adsorption of sodium oleate on the mineral surface was also affected.

3.3. Analysis of infrared (IR) spectra

Fig. 11 shows the infrared spectrum recorded with sodium oleate. The absorption peaks at 2929.73 cm^{-1} and 2851.87 cm^{-1} were attributed to the symmetrical stretching vibrations of the hydrocarbon bonds in $-\text{CH}_3-$ and $-\text{CH}_2-$. The absorption peaks at 1653.52 cm^{-1} , 1560.27 cm^{-1} , 1445.29 cm^{-1} , and 1424.56 cm^{-1} corresponded to the characteristic absorption peaks of the carboxylate ion. The peaks at 1560.27 cm^{-1} , 1445.29 cm^{-1} , and 1424.56 cm^{-1} were ascribed to the symmetrical stretching vibrations of the COO^- ions. In addition, the absorption peak at 721.80 cm^{-1} corresponded to the in-plane bending vibrations of -

COO⁻ [25]. In the infrared spectrum of CMC, the peak at 3440.55 cm⁻¹ was ascribed to the stretching vibration of -OH and the peak at 2920.35 cm⁻¹ was ascribed to the antisymmetric and symmetric bending vibrations of -CH₃ and -CH₂. The peaks observed at 1615.14 cm⁻¹ and 1421.46 cm⁻¹ corresponded to the antisymmetric stretching and symmetric stretching vibrations of -COO⁻, respectively. The characteristic absorption peak of -C-O-C- was observed at 1121.46 cm⁻¹. The peaks at 1057.91 cm⁻¹ and 1019.05 cm⁻¹ were ascribed to the stretching vibrations of the C-O bond in the primary and secondary alcohol groups, respectively. The peak at 3437.32 cm⁻¹ was ascribed to the stretching vibration of the -OH group present in CMC. The two peaks at 1604.10 cm⁻¹ and 1420.25 cm⁻¹ corresponded to the antisymmetric and symmetric stretching vibrations of -COO⁻ in the CMC molecule. The main polar groups of CMC were the hydroxyl (-OH) and carboxyl (-COOH) groups (Qin et al., 2012; Gong et al., 2018).

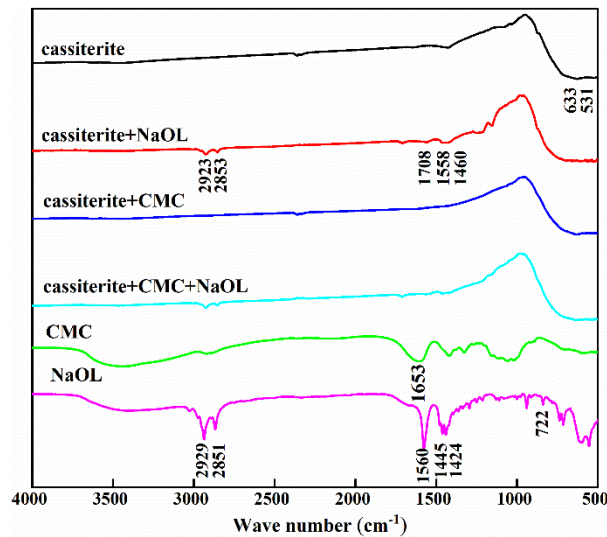


Fig. 11. Infrared spectral profiles of cassiterite, CMC, sodium oleate, and the interaction product

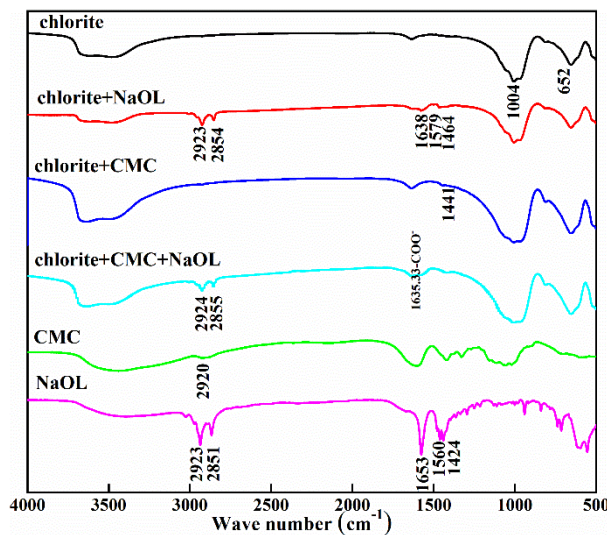


Fig. 12. Infrared spectral profiles of chlorite, CMC, sodium oleate, and the interaction product

Fig. 11 shows the infrared spectral profiles recorded with cassiterite under different conditions. The absorption peaks at 531.14 cm⁻¹ and 632.94 cm⁻¹ were ascribed to the two Sn-O vibrational frequencies (Peng et al., 2017; Zheng et al., 2018). New characteristic peaks appeared at 2923.58 cm⁻¹ and 2853.56 cm⁻¹ in the spectra recorded with sodium oleate when cassiterite reacted with sodium oleate. These peaks corresponded to the symmetric stretching vibrations of -CH₃- and -CH₂-, respectively. The characteristic peaks at 1708.80 cm⁻¹, 1558.64 cm⁻¹, and 1460.72 cm⁻¹ were ascribed to the vibrations of the COO⁻ group, caused by the interaction between the carboxylate ion (COO⁻) and the cassiterite surface.

The characteristic Sn-O peak shifted by 5.91 cm^{-1} , which indicated that the -COO- group in sodium oleate was chemically bonded to Sn-O at 531.14 cm^{-1} . The addition of CMC did not significantly change the position of the characteristic peaks of cassiterite. The zeta potential analysis revealed that CMC was adsorbed on the cassiterite surface (weak physical adsorption). New peaks appeared at 2924.05 cm^{-1} and 2853.67 cm^{-1} when cassiterite reacted with CMC and sodium oleate. The antisymmetric and symmetric stretching vibrational peaks of the methyl group corresponded to the symmetric stretching vibrational peaks of the -CH₃- and -CH₂- units in the spectra recorded with sodium oleate. Peaks corresponding to -COO- appeared at 1710.56 cm^{-1} and 1463.82 cm^{-1} . The peak corresponding to group vibration was ascribed to the interaction between the -COO- unit in sodium oleate and the cassiterite surface. Compared to the signals observed in the infrared spectrum of cassiterite with sodium oleate, the intensities of the peaks corresponding to the -COO- group on the cassiterite surface decreased when CMC was added to it. It indicated that CMC weakened the adsorption interaction between sodium oleate and the cassiterite surface. However, the effect was weak.

Fig. 12 shows the infrared spectral profile of chlorite. The absorption peaks at 3617.22 cm^{-1} and 3482.25 cm^{-1} were ascribed to the absorption peaks of the -OH group. The absorption peak at 1008.84 cm^{-1} corresponded to the stretching vibration of the Si-O bond. The absorption peak at 459.83 cm^{-1} corresponded to the bending vibration of the Si-O peak. The absorption peak at 652.82 cm^{-1} was ascribed to the characteristic absorption peak of Si-O-Si (Al) (Zheng et al., 2018; Qi et al., 1996). The infrared spectra of chlorite in the presence of sodium oleate exhibited new characteristic peaks at 2923.85 cm^{-1} and 2854.45 cm^{-1} . The antisymmetric and symmetric stretching vibrations of the methyl group corresponded to the symmetric stretching vibrations of -CH₃- and -CH₂- units, as seen in the infrared spectrum of sodium oleate. The peaks at 1653.52 cm^{-1} , 1560.27 cm^{-1} , and 1445.29 cm^{-1} were ascribed to the -COO- group vibrations caused by the interaction between the -COO- group in sodium oleate and CMC with chlorite surface.

A strong peak at 3645.25 cm^{-1} corresponding to the -OH group appeared in the spectrum recorded with the sample where CMC interacted with chlorite. At the same time, the spectrum of chlorite exhibited a new absorption peak at 1441.09 cm^{-1} . This was due to the chemical interaction between the -COO- group and the chlorite surface in CMC. However, the absorption peak was weak in intensity, and the area under the peak was small. It indicated that the strengths of the chemical interactions present between -COO- and the chlorite surface were weak. A shift in the stretching vibration of the Si-O bond, which appeared at 1008.84 cm^{-1} , was observed. The results from flotation tests, zeta potential experiments, and the analysis of literature reports revealed that CMC gets adsorbed on the chlorite surface via hydrogen bonding and weak chemical adsorption interactions.

3.4. XPS analysis

Fig. 13 shows the XPS spectra of the untreated cassiterite surface as well as that of the cassiterite surface treated with different agents (Sn3d, O1s, and C1s). Characteristic peaks of Sn3d and O1s were observed when the spectra were recorded with the untreated cassiterite samples. The peaks corresponding to C1s were attributed to environmental pollution. The C1s peak intensity was higher for the cassiterite sample treated with sodium oleate (compared to the untreated cassiterite). The intensity of the C1s peak on the surface of cassiterite treated by CMC was comparable to the intensity of the C1s peak for the sample not treated by medicament. This indicated that sodium oleate exerted a stronger effect on the cassiterite surface (compared to CMC). The results agreed well with the results obtained from the zeta potential experiments.

Fig. 14 shows the XPS spectra corresponding to the untreated chlorite surface and the spectra of the chlorite surface treated with different reagents (including Mg2p, Al2p, Si2p, O1s, and C1s). Characteristic peaks corresponding to Mg2p, Al2p, Si2p, Ca2p, and O1s were observed in the XPS spectra of the untreated chlorite sample. The peaks corresponding to C1s were believed to have originated due to environmental pollution. The intensity of the C1s peak originating from the surface of chlorite treated with sodium oleate was higher than that of the peak originating from the surface of the untreated chlorite sample. The intensity of the C1s peak originating from the chlorite surface treated by CMC was higher than that arising from the chlorite surface treated with sodium oleate. This indicated that both the agents could get adsorbed on the chlorite surface.

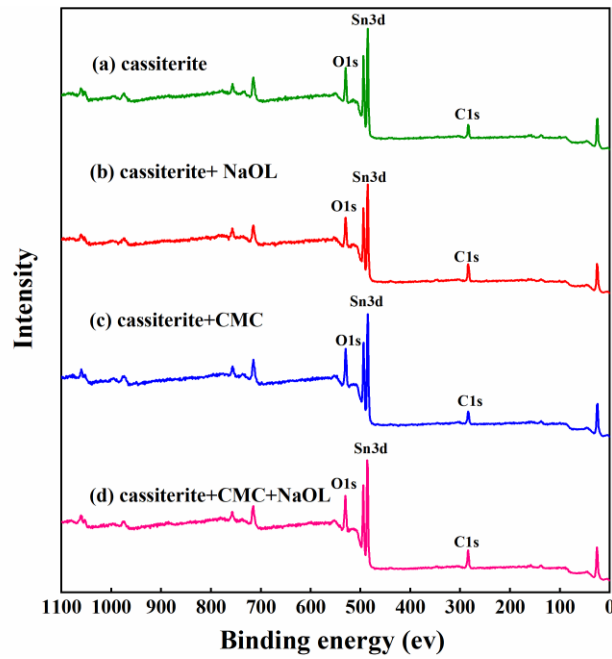


Fig. 13. XPS spectra of (a) untreated cassiterite, (b) cassiterite treated with sodium oleate, (c) cassiterite treated with CMC, and (d) cassiterite treated with sodium oleate and CMC

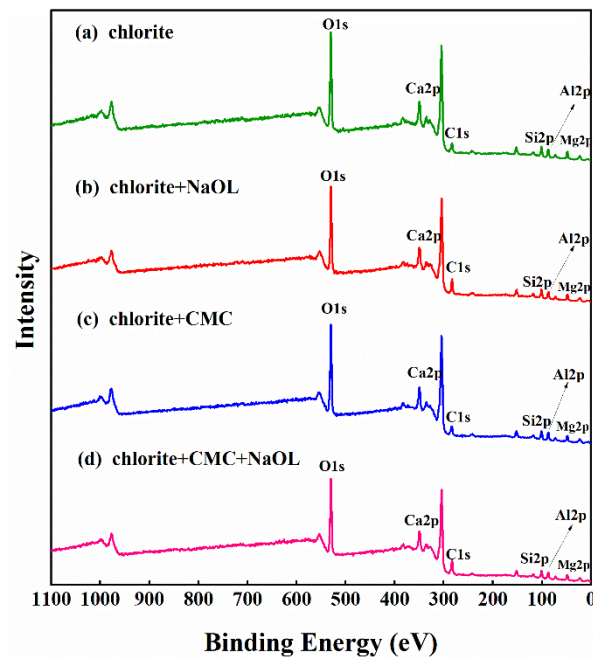


Fig. 14. XPS spectra of (a) untreated chlorite, (b) chlorite treated with sodium oleate, (c) chlorite treated with CMC, and (d) chlorite treated with sodium oleate and CMC

The concentrations of elements on the cassiterite surface treated with different chemical agents and the untreated cassiterite surface are shown in Fig. 15. When treated with two different reagents, the concentration of Sn on the cassiterite surface slightly changed. The concentration of the O element decreased by 2.95% when the surface was treated with sodium oleate, and the concentration of O decreased by 1.54% when the surface was jointly treated with CMC and sodium oleate. The concentration of C on the surface of cassiterite decreased when CMC was added to the pulp solution. The concentration of C increased by 3.83% when sodium oleate was added. The concentration of C increased by 2.53% when the surface interacted with CMC and sodium oleate. It showed that the addition of CMC could lower the extent of sodium oleate adsorption on the cassiterite surface.

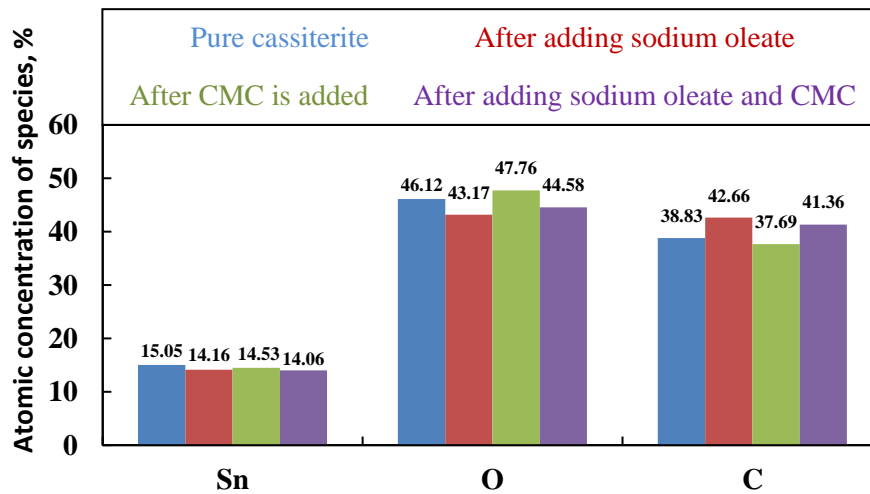


Fig. 15. Mole concentration of elements on the cassiterite surface

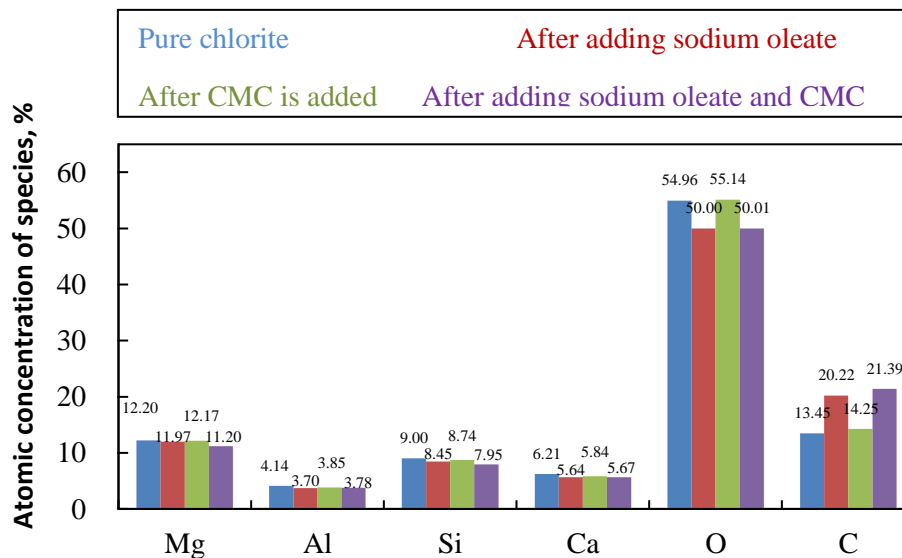


Fig. 16. Mole concentrations of elements on the chlorite surface

The concentrations of the elements on the surface of treated and untreated chlorite are shown in Fig. 16. When the sample was treated with two different agents, the atomic concentration of the elements on the surface of chlorite changed significantly. It is noteworthy that the concentration of C was significantly high. A comparison between Fig. 15 and 16 reveals that more amounts of sodium oleate get adsorbed on the surface of chlorite when sodium oleate is added to the system under study. The concentration of C increased by 6.8%. When CMC was added, the adsorption on the chlorite surface was less, and the concentration of C increased by 0.8%. The adsorption on the surface of chlorite increased by 7.9% when the two reagents were added.

A comparison of Figs. 15 and 16 reveals that the concentration of C on the surface of the two minerals increased when sodium oleate was added. It indicated that sodium oleate gets adsorbed on both the mineral surfaces. Hence, both the minerals can float upwards. The concentration of C on the cassiterite surface decreased, while the concentration of C on the chlorite surface increased. CMC gets adsorbed on the chlorite surface. However, a significant effect on the cassiterite surface was not observed when CMC was added to the pulp solution.

The Sn3d peaks originating from the surface of chemically treated cassiterite are shown in Fig. 17. The Sn3d spectrum of the pure cassiterite surface exhibited two characteristic peaks of the element. The first band at 486.28 eV corresponded to Sn3d_{5/2} and the second band at 494.70 eV corresponded to

Sn3d_{3/2} (Fig. 17a). The binding energy (of Sn3d) increased by 0.07 eV when treated with sodium oleate and that of Sn3d decreased by 0.17 eV when treated with CMC. The Sn3d binding energies differed by 0.2 eV post chemical treatment (Fig. 17b,c). The results revealed a weak interaction (or absence of interaction) between sodium oleate, CMC, and Sn sites on the cassiterite surface. The binding energies of the Sn sites on the cassiterite surface decreased by 0.04 eV under the combined action of the two agents. No significant change was observed (Fig. 17d). This indicated that the activity of the Sn sites on the cassiterite surface was low and they hardly participated in the reaction. It also revealed that sodium oleate and CMC could interact directly with the Sn sites on the cassiterite surface and get adsorbed.

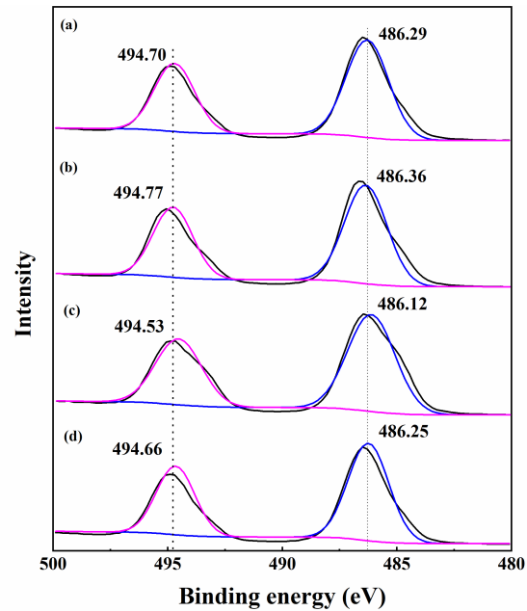


Fig. 17. Sn3d XPS peaks of (a) untreated cassiterite, (b) cassiterite treated with sodium oleate, (c) cassiterite treated with CMC, and (d) cassiterite treated with sodium oleate and CMC

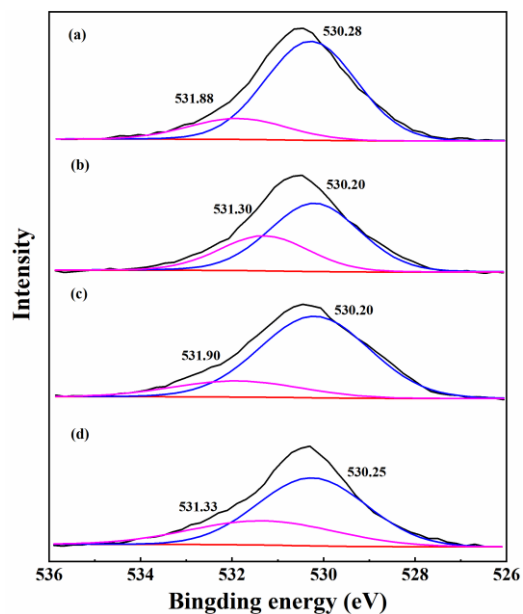


Fig. 18. O1s XPS peaks of (a) untreated cassiterite, (b) cassiterite treated with sodium oleate, (c) cassiterite treated with CMC, and (d) cassiterite treated with sodium oleate and CMC

The O1s spectra (for the treated cassiterite surface) are shown in Fig. 18. The O1s spectrum corresponding to the untreated cassiterite surface consisted of two peaks with electron binding energies of 530.28 eV and 531.88 eV (Fig. 18a). The peak at 530.28 eV represented the electronic binding energy

of the oxygen atom in the cassiterite lattice. The other peak at 531.88 eV represented the binding energy of the oxygen atom in the hydroxyl compound (Sn-OH) produced by surface hydroxylation of cassiterite (Li et al., 2008; Peng et al., 1985; Feng et al., 2017; Chen et al., 2017; Qicheng et al., 2018; Huang et al., 2019; Ren et al., 2017). When the cassiterite surface was treated with sodium oleate, it was observed that the binding energy of the oxygen atom in the cassiterite lattice changed from 530.28 eV to 530.20 eV. In comparison, the binding energy of the oxygen atom in Sn-OH changed from 531.88 eV to 531.30 eV (shifted by 0.58 eV, Fig. 18b). It indicated that the adsorption of sodium oleate on the surface of cassiterite changed the chemical nature of the oxygen atoms in Sn-OH. The O site in Sn-OH was the main reaction site of sodium oleate and the cassiterite surface. The two binding energy peaks for O1s (both within 0.1 eV) were observed in the spectral profile due to the interaction between CMC and the cassiterite surface (Fig. 18c). The results indicated a weak interaction between CMC and the O site of the cassiterite surface. When CMC and sodium oleate interacted on the cassiterite surface, it was observed that the oxygen atom binding energy in cassiterite lattice decreased by 0.03 eV and the oxygen atom binding energy in Sn-OH decreased by 0.55 eV (Fig. 18d). The chemical environment changed, which indicated that O in Sn-OH was the primary reaction site for sodium oleate and the cassiterite surface. However, CMC did not interact with the O site.

4. Conclusion

1. In the sodium oleate system, cassiterite has the best floatability in a weak alkaline environment. The chlorite floatability was better in an alkaline environment. When the sodium oleate dosage was 1×10^{-4} mol/L at pH 8, the cassiterite recovery was 87.89% and chlorite recovery was 29.3%. When CMC is added to the slurry, CMC has a stronger inhibitory effect on chlorite and a weaker inhibitory effect on cassiterite. When the CMC dosage was 12.5 mg/L at pH 8, the cassiterite and chlorite recoveries were 92.2% and 6.2%, respectively. The artificial mixed ore test revealed that the recovery of the mixed concentrate was 56.5%, the Sn grade was 60.12%, and the recovery was 85.2% in the absence of a depressant. When the CMC dosage was 6.5 mg/L, the best flotation separation was achieved. The mixed concentrate yield was 43.9%, Sn grade was 75.1%, and the recovery was 82.8%.
2. The potential measurements and infrared spectra revealed that sodium oleate could collect cassiterite and chlorite because it reacts with the surface of cassiterite and chlorite (via the chemical adsorption process). XPS spectral profiles revealed that the interaction between sodium oleate and the cassiterite surface was not realized through the Sn sites on the surface of cassiterite but through the surface hydroxyl groups. The results revealed that the oxygen sites in the hydroxyl compounds (Sn-OH) were generated due to these reactions. CMC did not interact with the oxygen sites. CMC had no effect on the flotation of cassiterite by sodium oleate as collector. But CMC can form hydrogen bonds with the chlorite surface. Weak chemical adsorption interactions between the carboxyl group in the CMC molecule and the metal cations on the chlorite surface were also observed. Thus, the interactions between sodium oleate and the chlorite surface and the flotation ability were affected, which resulted in the efficient separation of cassiterite and chlorite.

References

- LIU, J., HAN, Y., ZHU, Y., CHEN, Y., 2014. *Research Status and Prospective on Separation Technology of Fine Cassiterite*. Metal Mine., 10, 76-81.
- ZHANG, F., YIN, T., ZHOU, N., 2014. *The Current Situation and Thinking of the Tin Ore Resources Development and Utilization All Over the World.*, Modern Mining. 36(10), 1683-1689.
- ANGADI, A., SREENIVAS, T., JEON, H., 2015. *A review of cassiterite beneficiation fundamentals and plant practices*. Miner. Eng., 70, 178-200.
- WATERS, E., HADLER, K., CILLIERS, J., 2015. *The flotation of fine particles using charged microbubbles*. Miner. Eng., 21, 918-923.
- GEORGE, P., NGUYEN, A., JAMESON, G., 2004. *Assessment of true flotation and entrainment in the flotation of submicron particles by fine bubbles*. Miner. Eng., 17, 847-853.
- CHEN, Y., TONG, X., FENG, D., XIE, X., 2018. *Effect of Al (III) Ions on the Separation of Cassiterite and Clinocllore Through Reverse Flotation*. Minerals, 8, 347.
- FENG, Q., WEN, S., ZHAO, W., CHEN, Y., 2018. *Effect of calcium ions on adsorption of sodium oleate onto cassiterite and quartz surfaces and implications for their flotation separation*. Sep. Purif. Technol. 200, 300-306.

- FENG, Q., WEN, S., ZHAO, W., CHEN, H., 2018. *Interaction mechanism of magnesium ions with cassiterite and quartz surfaces and its response to flotation separation*. Sep. Purif. Technol. 206, 239-246.
- BEATTIE, V., DUTEROUE, J., 1992. *Flotation separation of arsenopyrite from pyrite*.
- WEI, Z., LIN, M., MU, X., LI, Y., 2015. *Flotation separation method of micro-fine-particle cassiterite minerals and quartz*.
- SUN, C., YIN, W., 2001. *Flotation principle of silicate minerals*. Beijing Science Press.
- AGNES. 1965. *Flotation of silicate and oxide*. China Industrial Press.
- LYUBIMOV, I., SHOKHIN, V., 1963. *Study of flotation properties of ilmenite and certain accessory minerals in ores from the Kusinskii deposit*. Nauch.Tr.Magnitogorsk Gorn. Inst. 33, 55–60.
- XU, YANG., QIN, W., 2012. *Surface Analysis of Cassiterite with Sodium Oleate in Aqueous Solution*. Separation science and Technology. 47, 502–506.
- BULATOVIC., SRDJAN, M., 2015. *Handbook of Flotation Reagents: Chemistry. Theory and Practice*.
- EJTEMAEIA, M., IRANNAJADA, M., GHARABAGHI, M., 2012. *Role of dissolved mineral species in selective flotation of smithsonite from quartz using oleate as collector*. International Journal of Mineral Processing. 114-117, 40-47.
- BURDUKOVA, E., LEERDAM, G., PRINS, F., SMEIK, R., LASKOWSKI, J., 2008. *Effect of calcium ions on the adsorption of CMC onto the basal planes of New York talc – A ToF-SIMS study*. Miner. Eng. 21, 1020-1025.
- ZHANG, J., 2010. *Effect of surfactant on Flotation of diaspore by sodium oleate*. Central South University.
- BULATOVIC., SRDJAN, M., 2015. *Handbook of Flotation Reagents: Chemistry, Theory and Practice*.
- WANG, J., SOMASUNDAM, P., 2005. *Adsorption and conformation of carboxymethyl cellulose at solid-liquid interfaces using spectroscopic, AFM and allied techniques*. Journal of Colloid and Interface Science. 291, 75–83.
- BEATTIE, D., HUYNH, L., GILLIAN, B., KAGGWA, J., 2006. *The effect of polysaccharides and polyacrylamides on the depression of talc and the flotation of sulphide minerals*. Miner. Eng. 19, 598–608.
- FENG, B., LU, Y., FENG, Q., ZHANG, M., GU, Y., 2012. *Talc—serpentine interactions and implications for talc depression*. Miner. Eng., 32, 68–73.
- XU, Y., AND QIN, W., 2012. *Surface Analysis of Cassiterite with Sodium Oleate in Aqueous Solution*. Separation Science and Technology, 47, 502–506.
- QIN, W., REN, L., XU, Y., WANG, P., MA, H., 2012. *Adsorption mechanism of mixed salicylhydroxamic acid and tributyl phosphate collectors in fine cassiterite electro-flotation system*. Journal of Central South University of Technology. 19, 1711-1717.
- GONG, G., HAN, Y., LIU, J., 2018. *Quantum Chemical Study of the Adsorption of NaOL on Cassiterite(211) Surface*. Journal of Northeastern University Natural Science. 39, 684-688.
- PENG, H., LUO, W., WU, D., BIE, X., SHAO, H., JIAO, W., LIU, K., 2017. *Study on the Effect of Fe³⁺ on Zircon Flotation Separation from Cassiterite Using Sodium Oleate as Collector*. Minerals, 7, 108.
- ZHENG, Z., LE, W., BO, Y., 2018. *Measurement of Carboxymethyl Cellulose by Thermal Infrared Spectroscopy*. Journal of Yili Normal University (Natural Science Edition).
- QI, B., XUE, Y., 1996. *Mechanism Study on the effect of carboxymethyl cellulose (CMC) on the flotation properties of gypsum and zinc hydroxide*. Foreign metal ore dressing, 05, 25–27.
- LIU, Y., SHEN, Z., DENG, J., JIANG, S., 2008. *Vibration spectrum characteristics and mineral genetic types of cassiterite*. Spectroscopy and spectral analysis, 28, 1506–1509.
- PENG, M., HE, S., 1985. *Infrared spectral study on cassiterite of different origins*. Chinese Science Bulletin., 12, 1655–1655.
- FENG, Q., ZHAO, W., WEN, S., CAO, Q., 2017. *Activation mechanism of lead ions in cassiterite flotation with salicylhydroxamic acid as collector*. Separation and Purification Technology., 178,193–199.
- CHEN, P., ZHAI, J., SUN, W., HU, Y., YIN, W., LAI, X., 2017. *Adsorption mechanism of lead ions at ilmenite/water interface and its influence on ilmenite flotability*. Journal of Industrial and Engineering Chemistry., 53, 285-293.
- HUANG, K., HUANG, X., JIA, Y., WANG, S., CAO, Z., ZHONG, H., 2019. *A novel surfactant styryl phosphonate mono-iso-octyl ester with improved adsorption capacity and hydrophobicity for cassiterite flotation*. Miner. Eng., 142, 105895.
- REN, L., QIU, H., QIN, W., HU, Y., 2017. *Flotation mechanism of cassiterite with octyl hydroxamic acid*. Journal of China University of mining and technology., 06, 187–194.
- LIU, C., ZHU, G., SONG, S., LI, H., *Flotation separation of smithsonite from quartz using calcium lignosulphonate as a depressant and sodium oleate as a collector*. 2019. Mine. Eng 131, 385–391.
- MENGJIE, T., SULTAN, A., WNG, L., SUN, W., ZHANG, C., HU, Y., 2019. *Selective separation behavior and its molecular mechanism of cassiterite from quartz using cupferron as a novel flotation collector with a lower dosage of Pb²⁺ ions*. Applied Surface Science., 486, 2280-238.